JOURNAL OF OPTOELECTRONICS AND ADVANCED MATERIALS Vol. 14, No. 11- 12, November – December 2012, p. 890 - 898

Simulating and modeling of three dimensional columnar growth nanosacle structure

R. S. DARIANI*, S. MINAEIFARD, M. RAJABI
Department of Physics, Alzahra University, Tehran, 19938, Iran

The mechanisms of nucleation and bulk growth in oblique angle deposition have recently attracted interest due to the formation of 3D columnar growth nanoscale structure. In this study, we present the results of growth simulation that explores the surface coverage of thin films during oblique angle deposition. The model is based on the deposition of incident particles directly under certain incident angle and particles surface diffusion. For computational efficiency, the potential is limited to nearest neighbor interactions. The model includes simulation of film growth from early growth stages of nucleation to later growth stages of columnar nanoscale structure.

(Received July 17, 2012; accepted October 30, 2012)

Keywords: Nucleation, Bulk growth, Surface coverage, Incident angle, Diffusion length

1. Introduction

In recent years, the study of nano-size materials generates intense interest because of their different promising properties that cannot be found in their bulk counterparts. Therefore, nanostructure formation and relations between growth conditions and physical properties are important research problems which have received much attention. There are different methods that have been used to fabricate nanostructures. One of them is the physical vapor deposition (PVD) [1] that atoms are deposited from a gas phase onto a substrate without decomposition of one chemical species into other species. The resulted layers from this method have different morphology due to stochastic and random deposition of particles within growth.

The oblique angle deposition is the extension of the commonly used PVD method. Experiments show that films deposited under an oblique angle of vapor incidence and at a moderate substrate temperature show a columnar morphology. The columns are inclined from the substrate normal toward the vapor incidence direction [2]. The oblique columnar thin films include many voids, and the spacing between the columns separated by these voids depends on the in-plane direction. Due to the shadowing effect, incident flux is preferentially deposited on the top of the highest surface features of the initial nucleation. This process only lets the highest islands to grow into columns and the isolated nano columns are tilting away from the surface normal to the incident evaporation beam direction. Shape, size, and column distribution of each column depends on different parameters. The parameters include deposition rate, deposition angle (i.e., the angle the velocity vector of a depositing atom makes with the substrate normal), the distribution of deposition angle (i.e., the degree of collimation of the deposition beam), the kinetic energy of the depositing atoms, the substrate temperature, etc [3]. The variation of column distribution and shape causes different optical, electrical, and magnetic properties in the structures. Not only electrical, magnetic, and optical but also chemical, medical, and biological applications of the thin films with the columnar structures are expected [4]. Therefore the nanostructure can be optimized for certain applications by controlling the deposition parameters.

An alternative way of to obtain controlled three dimensional (3D) nanoscale structure thin films is the glancing angle deposition (GLAD) method, which applies oblique angle deposition and substrate motion [5]. In this method within the growth process, the substrate rotates with controllable velocity about two axes which one of them is parallel to substrate and the other one is perpendicular to the substrate. Variation of the incident angle and substrate rotation leads to the formation of different nanostructured thin films such as chevrons, zig-zags, pillars, and helical columns. The structures clearly exhibit different physical properties and also have different applications.

Many applications have yet to be explored. Proposed applications of GLAD films include: electroluminescent devices, optically transparent conducting films sculptured from pure metals, optical sensors, optical coatings, thermoelectric materials, quantum effect devices, field emitters, and solar cells [6]. Computer simulations of columnar growth can greatly contribute to our understanding of the morphology and the physical properties of films as a function of deposition conditions.

Most of the models developed to predict film morphologies are based on continuum methods. In these methods, the evolution of the film surface is governed by a set of differential equations. The most common type uses string algorithm that the surface is exhibited by one or more strings in it. A number of such simulators are described in the literature, like SPEEDIE, SAMPLE, EVOLVE, and DEPICT [7]. Although there are many advantages to continuum models, they are difficult to

include atomic growth of layers in the models. For example, the stochastic processes lead to surface roughening.

The second type of simulators is based on stochastic and random processes like Monte Carlo (MC) model. In this model, most of random processes such as deposition and surface diffusion are simulated directly. SIMBAD is one of these simulators based on atomic MC model with ballistic trajectories [8]. The simulator is attempted to derive an expression for the column orientation and film density.

VFIGS is another 3D simulator that is based on two stages: the MC ballistic deposition process and surface diffusion [9]. The simulator is used for studying the effective surface area, packing density, and photocatalytic properties. Also, the simulator reproduces the measured optical response of fabricated rugate filters very accurately and explains measured features of the optical transmission spectra [10].

One of the 3D simulators is ADEPT that includes two basic events in the current level of implementation: the deposition event and surface diffusion [7]. The model can be used for materials that the provided atomic level information is due to the energies of atoms in representative surface configurations. Other simulators based on discontinues models were also designed such as 3d-films [11] for certain applications.

In this paper, we presented a model for the simulation of columnar nanostructure by PVD method. The model is based on two events a) deposition of incident particles directly under certain incident angle and b) particles surface diffusion. For computational efficiency, the potential is limited to nearest neighbor interactions.

The model includes simulation of film growth from early growth stages that 2D islands form on substrate surface (nucleation) until later growth stages that consist of columnar structures formation take part.

In addition to the 3D film growth simulation using this model, we have reviewed morphology of growing film at different stages of growth process. However, we have studied variations effect of some parameters such as; incident angle, diffusion length, and surface coverage on film structure at the end of nucleation stage and during columns growing. The details and results have been presented in the following sections.

2. Model description

Our simulation modeling of nanostructure growth by oblique angle deposition consists of two stages: nucleation and bulk growth. The model involved a 3D cubic lattice of size L×L×M with periodic boundary conditions. We considered that each particle has the dimension of one lattice point. The sites of lattice could be either occupied or unoccupied by particles. Each site should be occupied by at most one particle so a particle can only jump or locate an unoccupied site.

At each step a particle is sent towards the surface of the growing layer from randomly selected point at certain height above the surface. The direction of travel is determined by the geometry of the deposition at each stage. Substrate surface is an x-y plane and it is assumes to have zero height. The plane was completely uniform and without impurity or holes before deposition of incident particle. After deposition, the particle can diffuse to another nearest neighbor location on substrate by random walks. Deposition and diffusion processes were defined differently at two stages: nucleation and bulk growth which will be explained in next section.

2.1 Nucleation

Thin layer growth starts when the first incident particles arrives in and is fixed on substrate surface. When incident particles arrive on a bare substrate, they initially occupy physisorbed states and diffuse over the surface. If they have enough energy to surpass the potential barrier at their current position, they bind to the substrate and become fixed in place. The probability of surpassing the barrier depends on the energy of adatom and on the size of the barrier, which in turn depends on the substrate surface and film materials and local geometry. For any surface/film/temperature combination there is also a finite, possibly very small, probability that adatom will be desorbed from the surface. Note in our model desorption probability has been ignored. However, adatoms can encounter to each other and form nuclei. Also, with enlarging nuclei, desorption probability decreases. When nuclei's size passes the critical size, it is fixed on the substrate surface.

At initial times, the islands are two-dimensional (2D). In our model also simulation begins by formation of 2D islands onto substrate surface with thickness of one lattice site. In this stage, adatoms randomly are created and begin to diffuse on substrate surface by random walks. The number of jumps in the random walk, D is related to the diffusion length which is a function of many deposition parameters including substrate temperature, source material and chamber pressure during deposition. This quantity is defined as [9]

$$D = \frac{2a}{\sqrt{3}} d \tag{1}$$

where a is the lattice spacing and d is diffusion variable. We assume that whenever a diffusing particle before D^{th} walk encounters a monomer, the particle stop diffusing and is fixed on its site and form a two-atom cluster. When a diffusing particle encounters an island is fixed on its site

and becomes part of the island. Otherwise, the particle after D^{th} walk stops and becomes a monomer. After a particle is frozen, another particle is created and within this procedure 2D islands form with different sizes and are randomly diffused on substrate surface. Some of these islands within growth are attached to each other and form a bigger island.

With attaching any particle to substrate surface, substrate becomes more nonuniform and this nonuniformity causes other next particles to be shifted toward monomers or growing islands. Therefore, in diffusion stage on substrate surface the unoccupied neighbor points are not similar and jumping probability to each neighbor is different. These probabilities are determined due to the interaction of potential between diffusing particle and frozen particles. We assume Lennard-Jones potential as the interaction potential.

Jumping probability of diffusing particle from i^{th} point to j^{th} unoccupied neighbor is derived from the following equation

$$p_{i\to j} = \frac{\exp(L_j)}{\sum_j \exp(L_j)} \qquad (2)$$

where L_j is the interaction potential between particle that is located at j^{th} site and the particles already existed on the surface. Σ_j is sum over all allowed points (unoccupied nearest neighbor of j^{th} point).

2.2 Bulk growth

When substrate surface coverage in nucleation stage reaches to the level that is determined by the program, nucleation is stopped and column growth with deposition particle begins. Particles are randomly created in x-y plane at height h above highest growing column. The particles follow a linear oblique trajectory assuming no collision with atoms in the direction of vapor incidence until they reach to growing column. The direction is determined by the geometrical deposition condition which is defined as angle between substrate surface normal and vapor incidence. Ballistic depositions of particles with oblique incident allow particles to overhang.

After attaching particles on columns tops, surface diffusion begins, i.e. any particle starts to walk toward unoccupied nearest neighbor. This walk before frozen is a random number between zero and D (Eq. 1). When a particle is frozen then another particle is created and emitted to substrate. The deposition and surface diffusion are repeated until column heights are reached to certain level that is determined by the program.

3. Result and discussion

3.1 Effect of surface coverage variations

One of the effective parameters on the formation of nanostructures is surface coverage. Surface coverage is defined as the ratio of occupied lattice units to total units in the end of nucleation stage. Fig. 1 reviews effect of surface coverage variations on four important quantities: number of islands, monomer number, size of largest island, and packing density. The first quantity is number of islands (NI) is formed at the end of nucleation stage which in Fig. 1-a its variation versus surface coverage (Θ) variations is shown. According to Fig. 1-a, the number of islands curve versus surface coverage has a maximum at about 0.6. On the other hand, the number of clusters increases with increasing surface coverage before maximum value but after maximum value number of islands reduced with increasing Θ. Next quantity is the monomer number (NM) which in Fig. 1-b its variation versus surface coverage variations is shown. This curve also has a maximum about $\Theta = 0.5$. Note that, between 0.5 and 0.6 the monomer number is decreasing but the number of islands is increasing. Another quantity is the size of largest island (Smax) which in Fig. 1-c its variation versus surface coverage variations is shown. As shown in the figure from $\Theta = 0.6$, the size of largest island rapidly increases which indicates after this Θ, the size of islands increases.

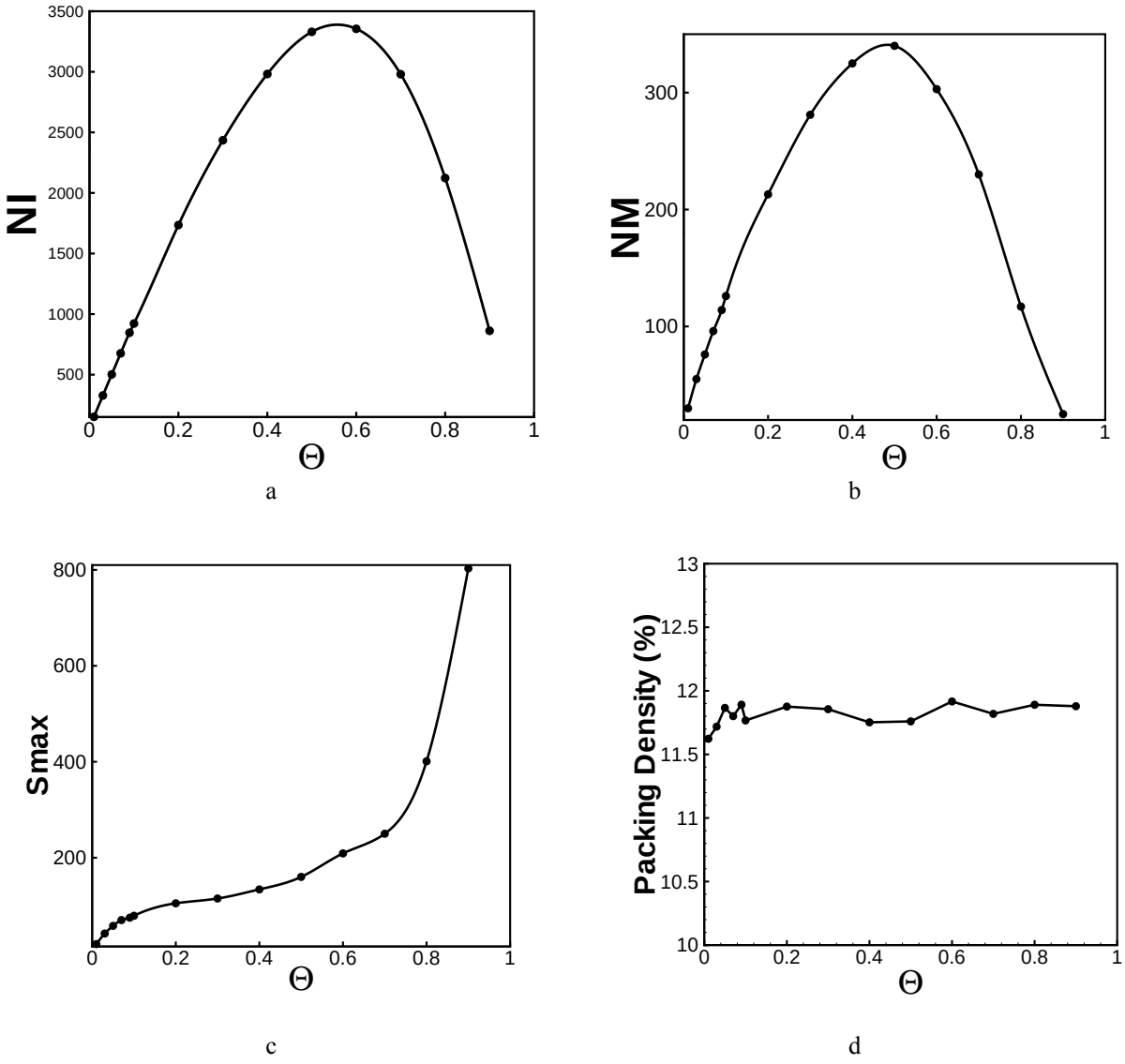

Fig. 1. (a) Number of islands versus surface coverage (b) Number of monomers versus surface coverage (c) Size of the largest island versus surface coverage (d) Packing density versus surface coverage. Above curves are taken in following conditions: α (incident angle) = 85°, d (diffusion length) = 2000, and h = 3.

It seems from figure 1-a and 1-c at incident angle 85° and diffusion length 2000 that when Θ reaches peak, system begins to coalescence stage. It means that the growing islands start attaching to each other and cause to decrease number of islands but the size of growing islands increases.

Up to now, surface coverage variations have been reviewed at nucleation stage. For studying the effect of variations on structural bulk growth, packing density variations as a function of surface coverage is shown in Fig. 1-d. Packing density is defined as ratio of occupied lattice units to total lattice units. As shown in the figure, packing density is not sensitive to Θ variations.

Fig. 2 reviews the shape and size of growing islands variations at nucleation stage. Figs. 2-a, 2-b, and 2-c show shape and size of islands on substrate surface (L = 300) at three different surface coverage.

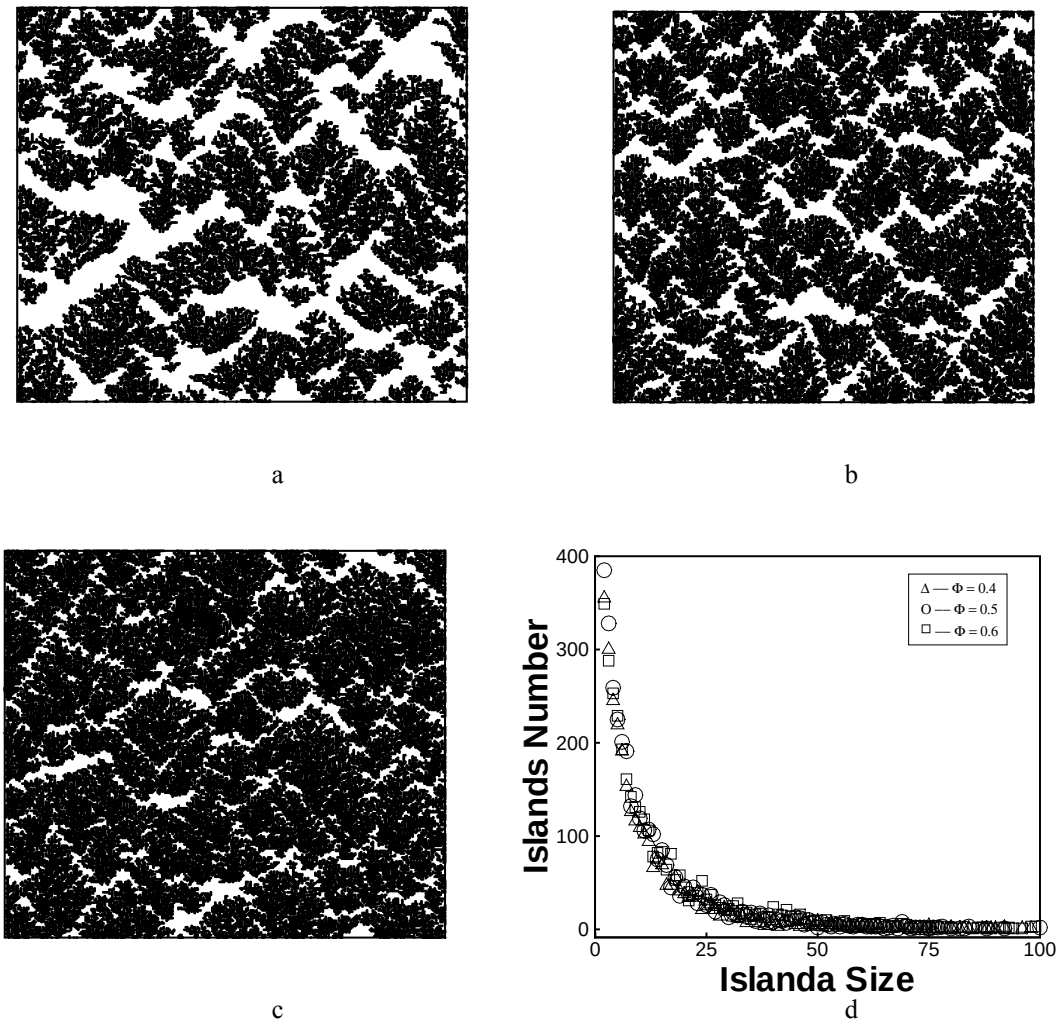

Fig. 2. Island morphology on 300×300 substrate is presented by our simulator. All cases are taken at α = 85˚, d = 2000, and h = 3. Island morphology are shown (a) at Θ = 0.4, (b) at Θ = 0.5, (c) and Θ = 0.6. (d) Island size distributions for them.

Fig. 2-d shows island size distribution respectively. Island size is the number of particles that formed the island.

As shown in the figures, island size distributions show approximately exponential behavior. At constant incident angle and diffusion length, the distributions behave as a function like below

$$y = ae^{-bx} \tag{3}$$

where a and b are coefficients that depend on surface coverage. In Fig. 3 variation of b as function of Θ reviewed. As shown in the figure, b decreases linearly with increasing Θ.

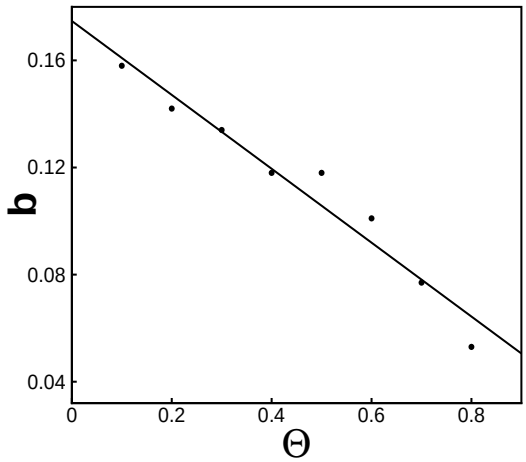

Fig. 3. Variation of b as function of surface coverage in following conditions: α = 85˚, d = 2000, and h = 3.

3.2 Effect of incident angle variations

Another effective parameter is incident angle (α) that has been reviewed on film growth in nucleation stage and also in columns bulk growth stage. Fig. 4 shows effect of incident angle variations on four important quantities. Figures 4-a, 4-b, and 4-c show effect of incident angle variations at the end of nucleation stage. The figures show the number of islands (NI), monomers (NM), and the size of the largest island (Smax) as a function of incident angle (α) respectively. According to our model, island height is exactly a lattice unit since our nucleation in this stage is totally two dimensional. Then, incident angle do not affect the above quantities and island morphology which are given in Fig.4.

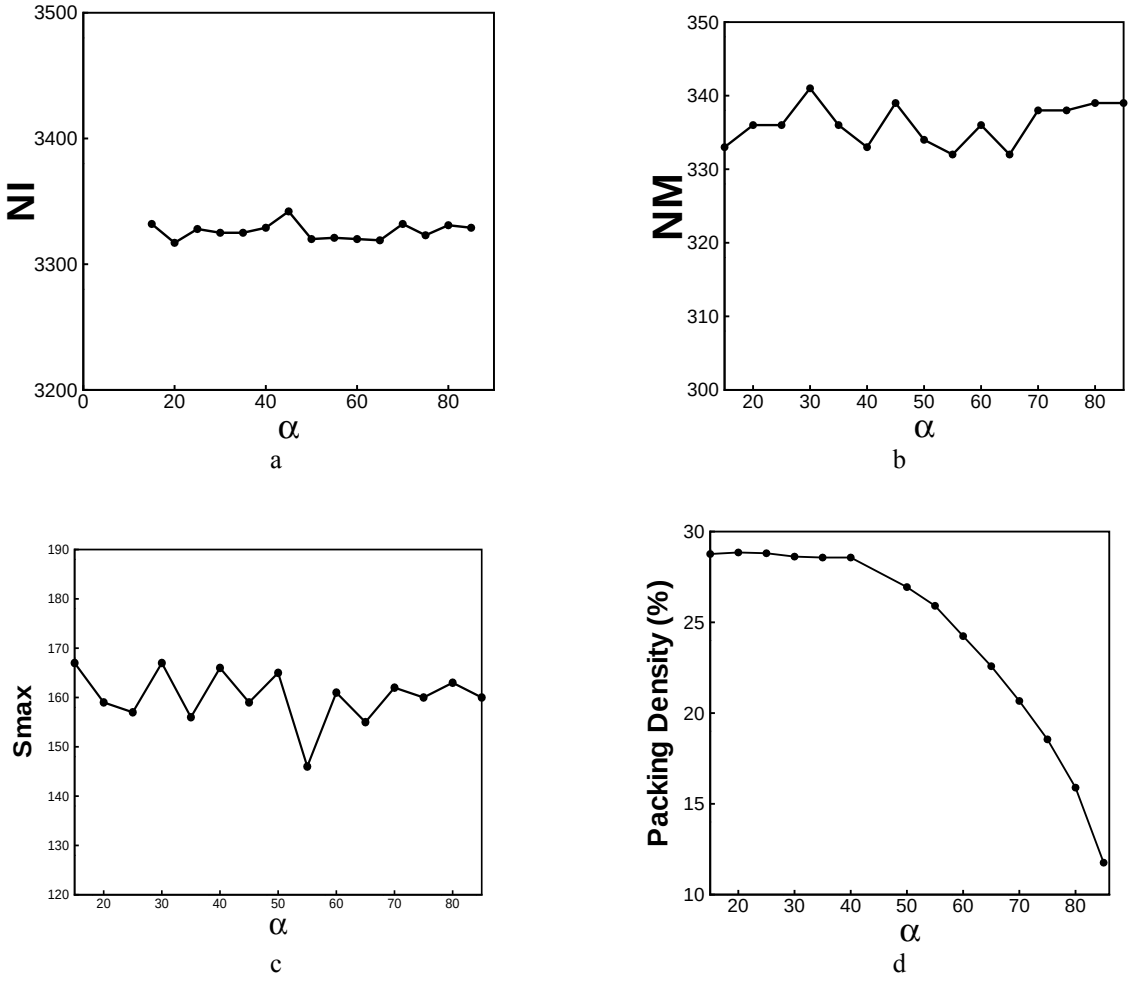

Fig. 4. (a) Number of islands versus incident angle (b) Number of monomers versus incident angle (c) Size of the largest island versus incident angle (d) Packing density versus incident angle. Above curves are taken in following conditions: surface coverage Θ = 0.5, diffusion length d = 2000, and h = 3 (α is in degree).

However, incident angle directly has considerable effect on columns properties and shape which its effect on packing density variations versus incident angle is shown at Fig. 4-d. As seen in the figure, packing density is reduced by increasing the incident angle.

One of the important effects of incident angle variation is on columns shapes that affect many film properties. Figures 5-a, 5-b and 5-c show that growing columns angle (β) strongly depends on particle incident angle (α) and β are increasing with increasing α. As already mentioned in the paper, two dominant phenomena on columns growth are surface diffusion and shadowing. Surface diffusion causes adatoms after incident on columns surface have the opportunity to move on the columns surface. Therefore adatoms shift toward corner points and cause more condensed structure. However, shadowing causes growing columns to shadow over certain regions of voids and prevents incident particles to reach to the voids and causes increasing voids between columns. In fact, at great incident angle (α>60˚) shadowing effect dominates surface diffusion. Therefore by increasing α, more oblique columns and voids are formed. But at small angle (α<60˚) surface diffusion dominates shadowing effect and as shown in the figure,

structure becomes more condensed. Note that at the small angles the shape columns will not be clear.

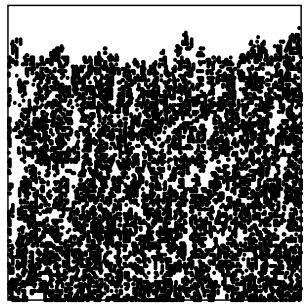

a

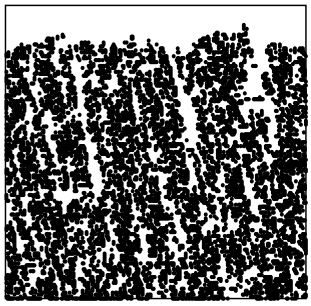

b

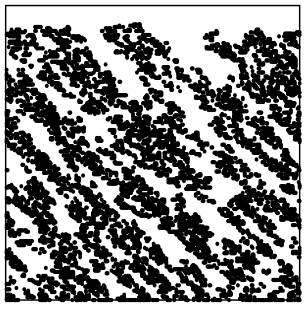

c

Fig. 5. Cross section of growth columns on 300×300 substrate are presented by our simulator. All cases are taken at Θ = 0.4, d = 2000, and h = 3. Cross section of growth columns are shown at α = 35˚ in Fig (a), at α = 60˚ in Fig (b), at α=80˚ in Fig (c).

3.3 Effect of diffusion length variations

Finally, diffusion length variations on growing structure are studied at two stages, nucleation and columns bulk growth were studied and results are shown in Fig.6 and Fig. 7. Fig. 6 shows variations of diffusion length four quantities; number of islands (NI) (Fig. 6-a), monomers (NM) (Fig. 6-b), size of largest island (Smax) (Fig. 6-c), and packing density (Fig. 6-d).

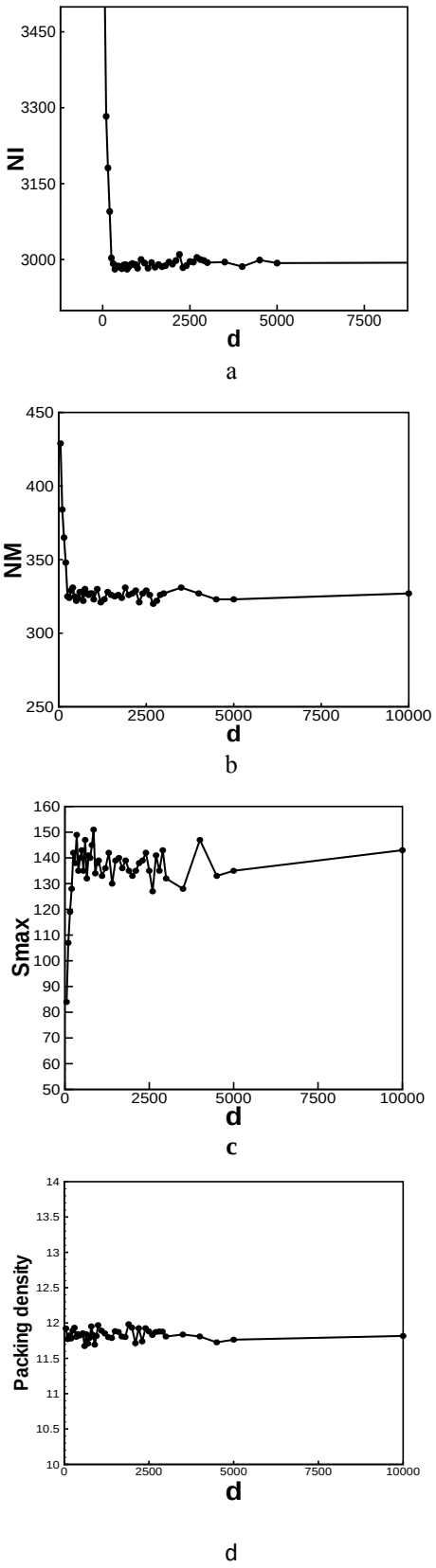

Fig. 6. (a) Number of islands versus diffusion length (b) Number of monomers versus diffusion length (c) Size of the largest island versus diffusion length (d) Packing density versus diffusion length. Above curves are taken in following conditions: α = 85˚, Θ = 0.4 and h =3.

Figs. 6-a and 6-b show by increasing diffusion length up to d = 1000, the number of islands and monomers strongly are reduced but after this point, both of them become almost constant. Fig. 6-c shows different behavior, i. e., up to d = 1000 size of largest island slowly increases and after this point becomes approximately constant. Fig. 6-d shows that packing density is not sensitive to diffusion length.

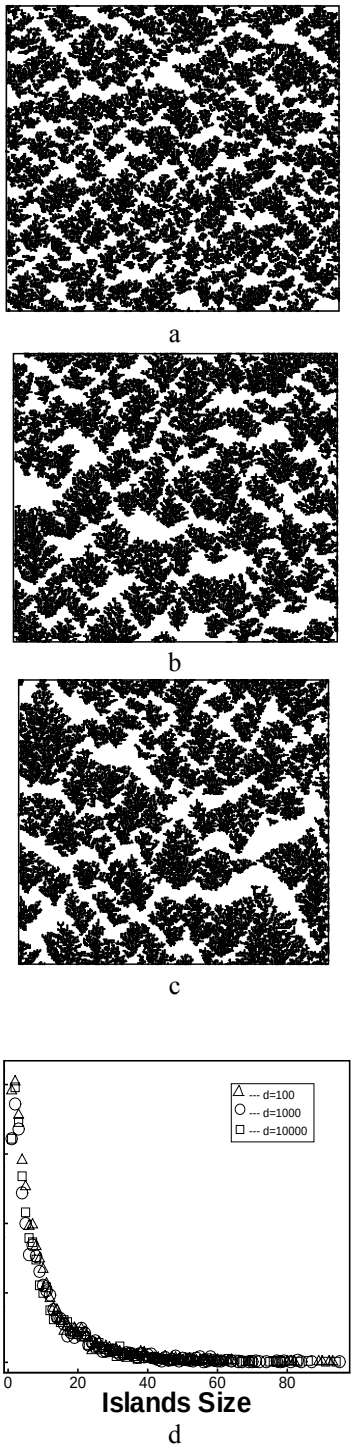

Fig. 7. Islands morphology on 300×300 substrate is presented by our simulator. All cases are taken at Θ=0.6, α = 85°, and h = 3. Island morphology are shown at d =100 in Fig (a), at d = 1000 in Fig (b), and at d=10000 in Fig (c). (d) Island size distributions for them.

Figs. 7-a, 7-b, and 7-c show island shape variation due to diffusion length variation. As shown in the figure, by increasing diffusion length, number of islands reduced and island dimension and distance between them one increased.

As shown in Fig. 7, island size distribution shows exponential behavior. The distribution in a constant incident angle and surface coverage shows similar behavior to Eq. 3. The interesting point is that island size and distance between islands increase by increasing diffusion length (see Fig. 7). However power b is not sensitive to variation of d and it has constant value (see Fig. 8).

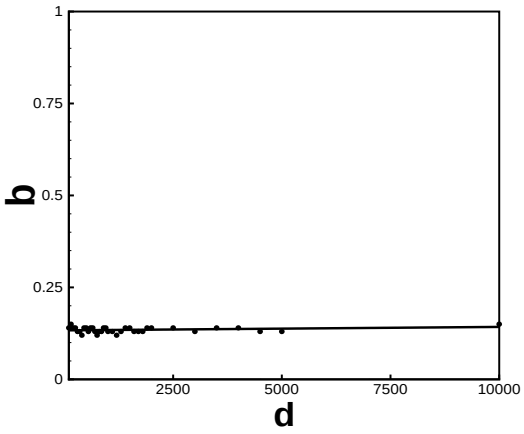

Fig. 8. Variation of power b in Eq. 3 versus diffusion length (d) in following conditions: Θ=0.6, α = 85°, and h = 3.

4. Conclusion

In conclusion, we have presented a detailed simulation study of growth dynamics during oblique angle deposition. The growth regimes have investigated surface coverage from early stages to final stages of nucleation. It has been shown that the number of islands and monomers versus surface coverage curves has a peak. The size of largest island increases by increasing surface coverage.

Our results also showed that packing density reduces by increasing incident angle, island sizes distribution is not sensitive to growing columns angle, and packing density is not sensitive to diffusion length. Increasing diffusion length does not affect columns shape and island size distribution.

Finally, we have extended the lattice MC model to simulate structure evolution during oblique angle deposition on a substrate. The phenomena of nucleation and bulk growth during the formation of columnar nanoscale structure are captured using our simulator.

Acknowledgements

We would like to acknowledge helpful assistants from Dr G. R. Jafari at Department of Physics, Shahid Beheshti University and Payam Norouzzadeh for useful discussions.

This work was financially supported by Alzahra University.

References

[1] Y. P. Zhao, D. X. Ye, G. C. Wang, T. M. Lu, SPIE Proceedings **5219**, 59 (2003).
[2] L. Abelmann, C. Lodder, Thin Solid Films **305,** 1 (1997).
[3] L. Dong, R. W. Smith, D. J. Srolovitz, J. Appl. Phys. **80**(10), 5682 (1996).
[4] A. Lakhtakia, R. Messier, M. J. Brett, K. Robbie, Innov. Mater. Res. **1**(1), 165 (1996).
[5] K. Robbie and M. J. Brett, J. Vac. Sci. Technol. A **15**, 1460 (1997).
[6] K. Robbie, G. Beydaghyan, T. Brown, C. Dean, J. Adams, C. Buzea, Rev. Sci. Instrum. **75**(4), 1089 (2004) -1097.
[7] H. Huang, G. H. Gilmer, T. D. De la Rubia, J. Appl. Phys. **84**(7), 3636 (1998).
[8] S. K. Dew, T. Smy, M. J. Brett, IEEE T. Electron Dev. **39**(7), 1599 (1992).
[9] M. Suzuki, Y. Taga, J. Appl. Phys. **90**(11), 5599 (2001).
[10] K. Kaminska, M. Suzuki, K. Kimura, Y. Taga, K. Robbie, J. Appl. Phys. **95**(6), 3055 (2004).
[11] T. Smy, D. Walkey, K. L. Harris, M. J. Brett, Thin Solid Films **391**, 88 (2001).

*Corresponding author: dariani@alzahra.ac.ir